

# Evolution of power sources for implantable cardioverter defibrillators

Ann M. Crespi, Sonja K. Somdahl, Craig L. Schmidt, Paul M. Skarstad\*

*Medtronic, Inc., 6700 Shingle Creek Parkway, Minneapolis, MN 55430, USA*

Received 18 December 2000; accepted 18 December 2000

## Abstract

The evolution of seven generations of power sources for implantable cardioverter defibrillators (ICD) is presented. The packaging efficiency of the power sources has steadily increased, resulting in smaller, lighter batteries while maintaining the required electrical characteristics. The main areas for improvement were reduction of headspace volume, reduction of separator volume, and a change from a two-cell battery to a single cell. © 2001 Published by Elsevier Science B.V.

*Keywords:* Applications/medical defibrillators; Lithium/silver vanadium oxide batteries

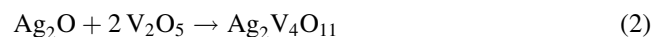
## 1. Introduction

Implantable cardioverter defibrillators (ICDs) are devices that treat very fast, and potentially lethal, cardiac arrhythmias. Implanted in the chest, these devices continuously monitor the heart's electrical signals and sense when the heart is beating dangerously fast. Within about 5–10 s, they deliver one or more electric shocks to return the heart to a normal rhythm. These shocks may range from a few microjoules to very powerful shocks of 25–40 J. The ICD is also capable of delivering continuous low-energy stimuli like a cardiac pacemaker.

The ICD battery must meet stringent requirements. To charge the capacitors that deliver the defibrillation shock, the battery must be capable of delivering about 50 J within about 5–10 s. A high-area electrode design is needed to meet this requirement. The battery must also deliver a continuous low current drain on the order of microamperes, and last for about 5–10 years. The performance of the battery must be highly predictable so that there is adequate warning before it is depleted. Finally, the battery must be very small so the ICD can be as small and comfortable as possible. Typical requirements for batteries for ICDs appear in Table 1.

Lithium/silver vanadium oxide batteries provide the high power, high energy density, and long-term stability required for ICDs and are the only type of battery used in ICDs today. They were invented about 20 years ago, and have continuously improved since then [1–14]. There are two distinct types of silver vanadium oxide (SVO) in use today. DSVO is

synthesized at about 380°C by the decomposition reaction in Eq. (1) [1,2]. CSVO is synthesized at about 500°C by the simple combination reaction shown in Eq. (2) [3].



Lithium/SVO batteries have a distinctive discharge curve with two plateaus, one at 3.24 V and another at 2.6 V. Fig. 1 shows the open-circuit voltage and area-normalized internal resistance of  $\text{Li/Li}_x\text{Ag}_2\text{V}_4\text{O}_{11}$  as a function of  $x$  (using CSVO). Studies have shown that between  $x = 0$  and 2 metallic silver appears in the CSVO cathode [15,16]. The appearance of metallic silver is associated with a decrease in the internal resistance of a Li/CSVO cell, as seen in Fig. 1. In this paper, the composition  $\text{Li}_{66}\text{Ag}_2\text{V}_4\text{O}_{11}$  will be considered as the fully discharged material. This composition corresponds to reduction of  $\text{Ag}^+$  to  $\text{Ag}^0$  and reduction of  $\text{V}^{5+}$  to  $\text{V}^{4+}$ . In order to maintain low times for charging the output capacitors of an ICD in practical use, batteries are not generally discharged to this degree of lithiation.

Until recently all ICDs were powered by two cells connected in series, doubling the voltage shown in Fig. 1. The circuitry used to power the device and to charge the capacitors has been improved so that many ICDs are now powered by a single cell. This change has greatly reduced the volume of the battery by reducing the volume of encasement material and other inactive components.

Two mechanical configurations have been described previously for Li/SVO batteries used in ICDs, one consisting of a multi-plate cathode and a lithium metal anode wound through the multi-plate cathode in a serpentine manner [6],

\* Corresponding author.

E-mail address: paul.skarstad@medtronic.com (P.M. Skarstad).

Table 1  
Requirements for batteries for implantable cardioverter–defibrillators

Battery requirement	Comments
Power	Must be capable of operating for several years at a background power of 50–100 $\mu$ W. In addition, must be capable of delivering 50–70 J pulses at a power greater than 4–10 W at any time on demand without delay
Energy	Typically about 20 kJ (5.56 Wh)
End-of-service indicator	A measurable battery parameter, such as voltage or resistance which indicates the need to replace the device
Size	Minimum size is required for ease of implant and patient comfort
Predictability	Long-term performance must be readily predictable from short-term data in order to project device longevity accurately
Reliability	The highest possible reliability is required for this life-saving application
Safety	The highest possible level of safety is required to protect the patient and medical personnel as well as manufacturing personnel who handle batteries

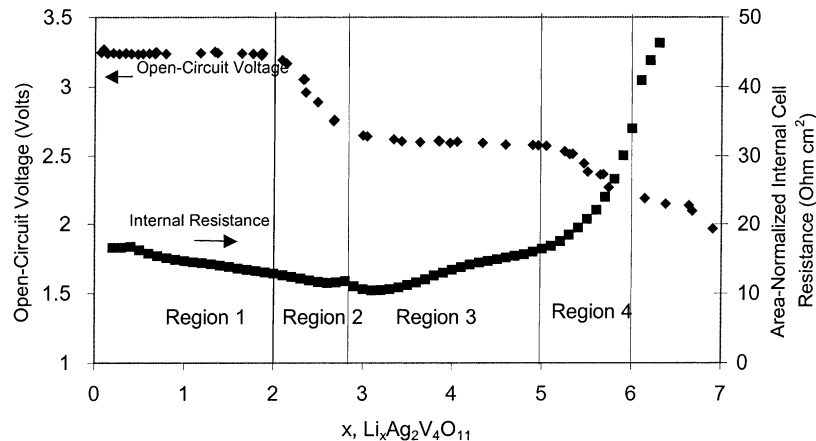


Fig. 1. Open-circuit potential and internal dc resistance of  $\text{Li}_x\text{Ag}_2\text{V}_4\text{O}_{11}$  (Li/CSVO) battery as a function of the extent of lithiation,  $x$ . The discharge curve is divided into four regions, where Region 1 is flat and extends from  $x = 0$  to 2; Region 2 slopes and extends from  $x = 2$  to 3; Region 3 is flat and extends from  $x = 3$  to 5; Region 4 slopes and extends from  $x = 5$  to 6.

the other consisting of a coiled electrode design. The designs described in this paper are all based on the coiled electrode configuration. Single strips of anode and cathode are wound into a flattened coil and inserted into a prismatic case.

A materials balance design model for high-rate, liquid electrolyte primary lithium batteries has been described [17]. This model consists of four equations that define the volumetric constraint, the electrode balance, the electrolyte requirement and the electrode loading. Solving the equations using matrix methods gives the anode and cathode capacities, the volume of electrolyte, and the dimensions of the electrodes. The lithium/CSVO batteries described in this paper, constructed according to this materials balance model, show consistent, predictable performance from design to design, despite wide variation in battery capacity, electrode loading and current density. A predictive model of battery voltage and resistance has been developed for these batteries [18].

### 1.1. Battery construction-general

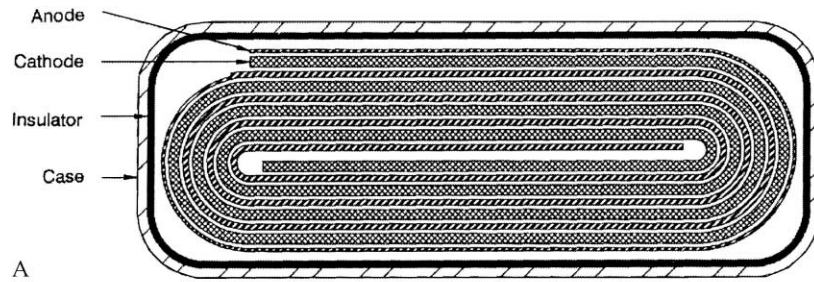
Batteries were assembled in hermetically sealed stainless steel cans with a lithium metal anode and an electrolyte consisting of 1 M  $\text{LiAsF}_6$  in a 1:1 mixture by volume of

propylene carbonate and 1,2-dimethoxyethane. The shape of the cans was usually a rectangular prism, but in Design VI one end of the cell was given a full radius, resulting in a “mailbox” shape. The cathodes were fabricated by mixing silver vanadium oxide ( $\text{Ag}_2\text{V}_4\text{O}_{11}$ ) with carbon and polytetrafluoroethylene then pressing onto a titanium mesh current collector [6]. The anodes were lithium metal pressed onto a nickel current collector. The anode and cathode were each encased in polypropylene separator, giving two layers of separator between the electrodes. The feedthrough consisted of a niobium wire within Ta23 glass. CSVO was synthesized as described in [1–3]. In all cell designs, the electrodes were wound together in a flattened coil. The designs were all case-negative. The electrode capacities, electrolyte volume, and electrode dimensions for each battery were calculated using the method in [18].

## 2. Design variants and their evolution

### 2.1. General description of design

The design of the ICD batteries is depicted in Fig. 2A and B. Fig. 2A is a cross-sectional view of the battery showing



A



B

Fig. 2. A cross-section view of the coiled electrode configuration (A). An assembly view of a typical battery with the cover and electrode coil partially removed showing the attachments in the headspace (B).

the coiled electrodes. The electrodes are wound into a flattened coil that fits the dimensions of the rectangular prismatic case. The polypropylene separator, which encases both electrodes, is not shown in this figure. Fig. 2B is an assembly view showing the connections of the electrodes to the feedthrough and case. The titanium current collector of the cathode is welded to the niobium feedthrough pin. The feedthrough is insulated with Ta23 glass. The nickel current collector of the anode is welded to the case wall. The case is lined with an insulator, except in areas close to the case-to-cover weld and the weld of the anode current collector to the case. The space between the top of the coil and the inside of the cover is termed the headspace. This volume is used to make connections to the electrodes while keeping features of

opposite polarity insulated from each other. The shapes of the batteries are illustrated in Fig. 3. Characteristics of seven designs are shown in Table 2.

The designs progress chronologically from left to right, showing improvements in volumetric efficiency with time. For medical devices such as the ICD, volumetric efficiency is considered more important than gravimetric efficiency, provided the device does not become unreasonably heavy. Therefore, this discussion will focus on volume rather than mass. The maximum power was calculated by equating the internal resistance of the battery and the resistance of the external load. This power is the instantaneous maximum power. It has been reported that under some conditions concentration polarization will reduce the available the

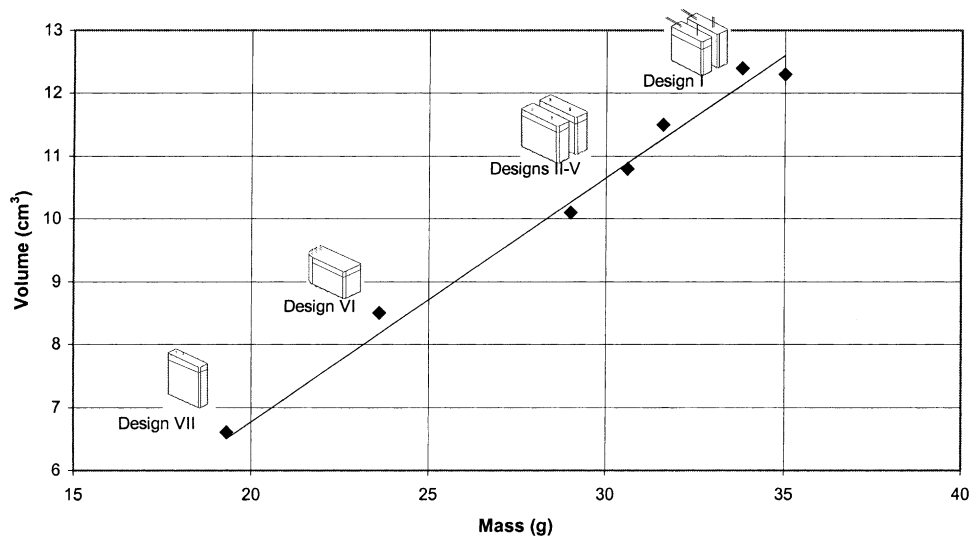


Fig. 3. The relationship between battery volume and mass with drawings of battery shapes. The solid line is a linear regression with an adjusted  $R^2$  of 0.983; intercept:  $-1.0 \text{ cm}^3$ ; slope:  $0.388 \text{ cm}^3 \text{ g}^{-1}$ .

Table 2  
Characteristics of the designs of seven defibrillator batteries<sup>a</sup>

Design	I	II	III	IV	V	VI	VII
External volume per battery ( $\text{cm}^3$ )	12.4	11.5	10.1	12.3	10.8	8.5	6.6
Mass per battery (g)	33.8	31.6	29.0	35.0	30.6	23.6	19.3
Capacity per cell (Ah)	0.93	0.92	0.092	1.15	1.04	1.77	1.35
Maximum power, zero discharge (W)	16.5	16.3	12.3	15.8	10.8	11.6	11.8
Gibbs energy density ( $\text{mWh cm}^{-3}$ or $\text{Wh dm}^{-3}$ )	427	454	515	531	549	590	579
Energy delivered to charge defibrillation capacitors (J)	70	70	58	70	50	65	58
Volumetric efficiency of utilized active components (%)	19.0	20.2	22.9	23.6	24.4	26.2	25.7
Volume of separator (inc. pores) as percentage of total volume (%)	23.1	23.8	21.8	22.6	19.0	21.5	8.5
Headspace (cm)	0.56	0.33	0.33	0.33	0.33	0.31	0.44
Cells per battery	2	2	2	2	2	1	1
Total separator thickness between electrodes (mm)	0.18	0.18	0.18	0.18	0.18	0.18	0.05

<sup>a</sup> Theoretical capacity is defined to a cathode composition of  $\text{Li}_6\text{Ag}_2\text{V}_4\text{O}_{11}$ .

power [19]. However, the effects of concentration polarization are not expected to differ much between battery designs, so the maximum instantaneous power is a valid point of comparison. Full discharge is defined as a cathode composition of  $\text{Li}_6\text{Ag}_2\text{V}_4\text{O}_{11}$ .

## 2.2. Reduction in volume of the headspace

The height of the headspace is measured as the distance between the top of the electrode coil to the inside surface of the cover. Design II was nearly identical to Design I, except the height of the headspace was reduced from 5.6 to 3.3 mm and the overall height of the battery was reduced accordingly. The volume of the battery was reduced by 7%. Design IV has nearly the same external dimensions as Design I, but height of the electrodes was increased to fill more of the headspace. The length of the electrodes was decreased to keep the electrode area nearly the same, and the loading was increased. The Gibbs energy density increased by 24% while

the power was only slightly reduced. Design III was designed for an ICD with lower-energy defibrillation capacitors. It has thicker electrodes with less area, resulting in lower power and higher Gibbs energy density. Design V was designed to charge even lower energy defibrillation capacitors, so it has further reduced power and increased energy density. The height of the headspace was increased slightly in Design VII due to geometric constraints of this particular design.

## 2.3. Progression from two cell to single cell design

For Designs I–V, all of the batteries consisted of two cells in series. After Design V, advances in the ICD circuitry for charging the defibrillation capacitors made it possible to use a single cell rather than two cells in series. The volumetric efficiency increased substantially in Design VI, a single cell battery, because less packaging material is needed for one cell compared to two cells. The electrode area and capacity

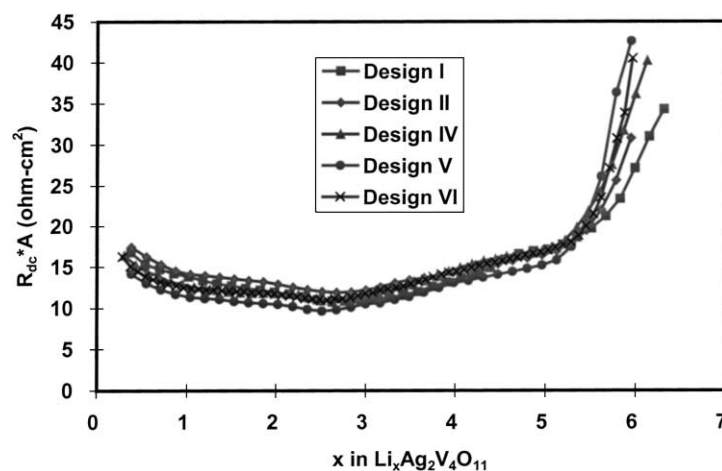


Fig. 4. Area-normalized dc resistance ( $R_{dc}$ ) as a function of degree of cathode lithiation for five of the battery designs. The resistance is calculated from the drop in voltage during a high current pulse using Ohm's law and normalized using the two-sided cathode area. The batteries were discharged on a low current drain for 1 year with a series of four high-current pulses applied every month. The  $R_{dc}$  was calculated using the voltage drop during the fourth pulse in each series. The data points displayed are interpolated for purposes of averaging data.

was increased by about 50% in the single-cell design compared to a two-cell battery.

#### 2.4. Reduction in volume of the separator

In Designs I–V, the separator, including pores, occupied 19–24% of the total volume of the battery (see Table 2). After reducing the volume of the headspace and changing to a single-cell battery it was clear that the volume of separator material must be reduced if the volume of the battery was to be reduced much more. In Design VII, the thickness of the separator was reduced from 0.09 to 0.025 mm per layer. When this change was made, the manufacturing line was moved to a clean room and processes were improved to prevent shorting across the thinner separator by foreign material. Burn-in and acceptance tests were changed to ensure detection of latent short-circuits which may occur when an oxidizable metal particle is present on the cathode. Production batteries were sampled frequently from the line, opened, and is inspected for evidence of foreign materials. The volume occupied by the separator was reduced to about 8% of the total volume of the battery.

### 3. Electrical and mechanical characteristics

The relationship between mass and volume for the battery designs is illustrated in Fig. 3. This graph shows that in spite of the many design changes, there is an excellent correlation between mass and volume. The average gravimetric density of the batteries is  $2.85 \text{ g cm}^{-3}$ . Finally, the electrical characteristics of this family of batteries remain consistent over the full range of designs with wide variation in electrode capacity, electrode loading and pulse-current density. Fig. 4 shows the area-normalized resistance versus degree of lithiation for five of the battery designs. Consistency of

design approach, embodied in the materials balance design model, helps to ensure scalable battery performance. Despite the many variations in design, battery resistance remains scalable by electrode area if battery capacity is presented as degree of lithiation.

### 4. Conclusions

Batteries for implantable defibrillators have been continually improved over time, resulting in lower volume, higher energy density, lower charging times and better packaging efficiency. These improvements have resulted in superior performance and smaller volumes for these devices.

### References

- [1] C.C. Liang, M.E. Bolster, R.M. Murphy, US Patent 4,310,609 (1982).
- [2] C.C. Liang, M.E. Bolster, R.M. Murphy, US Patent 4,391,729 (1983).
- [3] A.M. Crespi, US Patent 5,221,453 (1993).
- [4] P.P. Keister, R.T. Mead, B.C. Muffoletto, E.S. Takeuchi, S.J. Ebel, M.A. Zelinsky, J.M. Greenwood, US Patent 4,830,940 (1989).
- [5] P.P. Keister, R.T. Mead, B.C. Muffoletto, E.S. Takeuchi, S.J. Ebel, M.A. Zelinsky, J.M. Greenwood, US Patent 4,964,877 (1990).
- [6] W.G. Howard, R.W. Keim, D.J. Weiss, A.M. Crespi, F.J. Berkowitz, P.M. Skarstad, US Patent 5,439,760 (1995).
- [7] E.S. Takeuchi, M.A. Zelinsky, P. Keister, in: Proceedings of the 32nd Power Sources Symposium, 1986, p. 268.
- [8] P.M. Skarstad, in: Proceedings of the 12th Annual Battery Conference on Applications and Advances IEEE 97Th8226, 1997, p. 151.
- [9] C.F. Holmes, P. Keister, E.S. Takeuchi, Prog. Batt. Solar Cells 6 (1987) 64.
- [10] E.S. Takeuchi, P. Piliero, J. Power Sources 21 (1987) 133.
- [11] W.C. Thiebolt III, E.S. Takeuchi, Abstract 20, p. 29, The Electrochemical Society Extended Abstracts, Vol. 87-2, Honolulu, HI, October 18–23, 1987.

- [12] E.S. Takeuchi, W.C. Thieboldt III, J. Electrochem. Soc. 135 (1988) 2691.
- [13] A.M. Crespi, P.M. Skarstad, J. Power Sources 43/44 (1993) 119.
- [14] A.M. Crespi, F.J. Berkowitz, R.C. Buchman, M.B. Ebner, W.G. Howard, R.E. Kraska, P.M. Skarstad, in: A. Attewell, T. Keily (Eds.), Power Sources, Vol. 15, International Power Sources Committee, Leatherhead, UK, 1995, p. 349.
- [15] A.M. Crespi, P.M. Skarstad, H.W. Zandbergen, J. Power Sources 54 (1995) 68.
- [16] K. West, A.M. Crespi, J. Power Sources 54 (1995) 334.
- [17] P.M. Skarstad, A.M. Crespi, C.L. Schmidt, D.F. Untereker, in: A. Attewell, T. Keily (Eds.), Power Sources, Vol. 14, International Power Sources Committee, Leatherhead, UK, 1993, p. 167.
- [18] A.M. Crespi, C.L. Schmidt, J. Norton, K. Chen, P.M. Skarstad, J. Electrochem. Soc., 148 (2001) A30–A37.
- [19] J.D. Norton, C.L. Schmidt, Electrochemical Society Proceedings, Vol. 97-18, (1997, Pennington, N.J.) pp. 389–393.